Scanning Tunneling Microscopy: A Unique Tool in the Study of Chirality, Dynamics, and Reactivity in Physisorbed Organic Monolayers

STEVEN DE FEYTER, ANDRÉ GESQUIÈRE, MOHAMED M. ABDEL-MOTTALEB, PETRUS C. M. GRIM, AND FRANS C. DE SCHRYVER*

Department of Chemistry, Katholieke Universiteit Leuven, Celestijnenlaan 200 F, B-3001 Heverlee, Belgium

CHRISTIAN MEINERS, MICHEL SIEFFERT, SURESH VALIYAVEETTIL, AND KLAUS MÜLLEN

Max-Planck-Institut für Polymerforschung, Ackermannweg 10, D-55128 Mainz, Germany

Received November 5, 1999

ABSTRACT

Scanning tunneling microscopy (STM) is applied to study organic monolayers, physisorbed at the liquid−graphite interface. Due to the very local nature of the probing, the structure of these adlayers has been imaged with very high detail. The high resolution allowed us to investigate the effect of molecular chirality on the monolayer formation and provided a unique way to study chemical reactions at the liquid−graphite interface. Making use of a fast scanning mode, dynamic processes in these adlayers have been visualized.

Introduction

The invention of the scanning tunneling microscope (STM) in the early 1980s[1,2] opened new ways to study surface phenomena on a molecular and even atomic scale due to the very localized nature of the probing. The initial applications of STM were focused on the imaging of semiconductor, inorganic, and metal surfaces. In the late 1980s, the potential of STM was demonstrated for the study of physisorbed organic molecules, "immobilized" by the formation of densely packed two-dimensional layers at the solid−liquid interface, first for liquid-crystalline compounds and later for non liquid crystals.[3−5] This efficient approach to reduce the mobility of molecules, a prerequisite for high-quality imaging, stimulated STM investigations under ambient conditions at the liquid−solid interface. The majority of these studies dealt with the factors controlling the two-dimensional ordering of molecules and the contrast mechanism (for reviews, see refs 6−8).

Beyond the mere determination of the two-dimensional (2D) ordering of monolayers, STM has the potential to provide insight into a broad field of topics such as chirality,[9−15] reactivity,[16−20] and dynamics[21−30] at interfaces on a (sub)molecular scale. Attracted by its potential, we among others have tried to illustrate the usefulness of STM as a unique analytical tool for the characterization of physisorbed monolayers.

To address these issues, we have chosen to investigate predominantly functionalized isophthalic and terephthalic acid derivatives. This choice was motivated by our experience with simple alkylated isophthalic and terephthalic acid derivatives, as will be demonstrated in the following section.

The Building Blocks: Isophthalic and Terephthalic Acid Derivatives

Physisorbed monolayers at the liquid−solid interface can be obtained by depositing a drop of a solution containing the compound to be studied on atomically flat substrates, e.g., highly oriented pyrolytic graphite (HOPG). Figure 1 presents the experimental setup for imaging this kind of monolayer at the liquid−graphite interface. Note that the tip (Pt/Ir) is immersed in the supernatant solution during scanning. It takes typically 7 s to acquire an image. None

Steven De Feyter graduated from K. U. Leuven, Belgium, in 1993. He obtained his Ph.D. degree in 1997 at the same university, where he undertook research with Frans De Schryver in the field of scanning tunneling microscopy. After a stay as a Fulbright fellow at the California Institute of Technology (Caltech) with Ahmed Zewail, he returned to Leuven.

André Gesquière graduated from K. U. Leuven in 1997. He is currently working on his Ph.D. in the group of Frans De Schryver on the characterization and chemistry of supramolecular structures on surfaces.

M. M. Abdel-Mottaleb received his B.Sc. degree in chemistry from Ain Shams University in 1997 and his M.Sc. degree in chemistry from K. U. Leuven in 1999, and he is currently working on his Ph.D., investigating dynamic processes in physisorbed monolayers.

Petrus C. M. Grim received his M.Sc. degree in physics from the University of Nijmegen, The Netherlands, in 1989. He obtained his Ph.D. degree from the University of Groningen. Currently, he is a postdoctoral researcher at K. U. Leuven.

Frans De Schryver obtained his doctoral degree at K. U. Leuven in 1964 and returned as staff member to his alma mater after a two-year postdoctoral stay as a Fulbright fellow at the University of Arizona with Speed Marvel. He became full professor in 1975, working in the field of photochemistry and photophysics. He received a Humboldt research award in 1993 and stayed with G. Wegner and J. P. Rabe at the Max-Planck-Institute for Polymer Research in Mainz. After this stay he combined space and time resolution in the study of organic molecules. He received the Porter medal in 1998 and the Havinga medal and Forster memorial lecture award in 1999.

Christian Meiners studied chemistry at the University of Bonn, Germany. He received his Ph.D. degree in 1998 for the investigation of supramolecular polymeric architectures in the group of Klaus Müllen.

Michel Sieffert received his Diploma "D.E.A." in chemistry from the University of Strasbourg in 1996 and is currently a Ph.D. student under Klaus Müllen.

Suresh Valiyaveettil obtained his B.Sc. degree and M.Sc. degree from the Calicult University in India. He moved to the University of Victoria, Canada, to complete his Ph.D. work with T. M. Fyles. From 1993 to 1997, he worked with Klaus Müllen. In 1998, he joined the chemistry department at the National University of Singapore as an assistant professor.

Klaus Müllen obtained a Diplom-Chemiker degree at the University of Cologne in 1969 after work with Professor E. Vogel. His Ph.D. degree was granted by the University of Basel, Switzerland, in 1972, where he undertook research with Professor F. Gerson. He received his habilitation from the ETH Zürich in 1977. In 1979 he became a Professor in the Department of Organic Chemistry, University of Cologne, and accepted an offer of a chair in Organic Chemistry at the University of Mainz in 1983. He joined the Max-Planck-Society in 1989 as one of the directors of the Max-Planck Institute for Polymer Research. In 1993 he was awarded the "Max-Planck-Forschungspreis" and in 1997 the "Philip Morris-Forschungspreis".

10.1021/ar970040g CCC: $19.00
Published on Web 05/31/2000

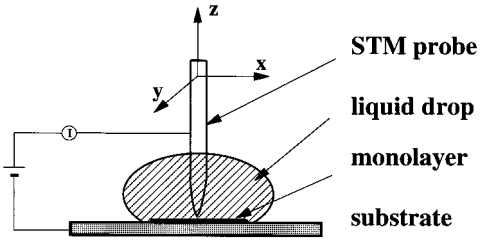

FIGURE 1. Experimental approach of STM in liquids.

of the images have been filtered, unless stated otherwise. A white frame in a STM image indicates the area represented by the corresponding model. Yellow parallelograms represent unit cells. All images are obtained in the constant height mode. Therefore, the image contrast reflects the changes in tunneling current at a constant bias voltage recorded during scanning of the sample. White corresponds to the highest and black to the lowest measured tunneling current. In general, variations in both topographic and electronic coupling properties of a molecular overlayer will influence the contrast of a STM image. Claypool et al. proposed a simple way to estimate the electronic tip−sample coupling on the basis of the ionization potential (IP):[31] if the coupling is dominated by the HOMO, functional groups with IPs lower than that of the corresponding alkane should appear bright, while functional groups with higher IPs should appear dark. This approach fails for some functional groups and if topographic factors dominate. The same authors developed a theoretical model based on perturbation theory, and computations suggest that the highly diffuse orbitals of the adsorbed molecules, despite being much farther in energy form the Fermi level of the graphite than the occupied orbitals, also play an important role.[32]

Figure 2A shows a STM image of a monolayer of 5-octadecyloxyisophthalic acid (**1**) physisorbed from 1-phenyloctane on the graphite surface.[17] The larger bright spots in this functionalized hydrocarbon monolayer correspond to the aromatic moieties. The darker regions in the image

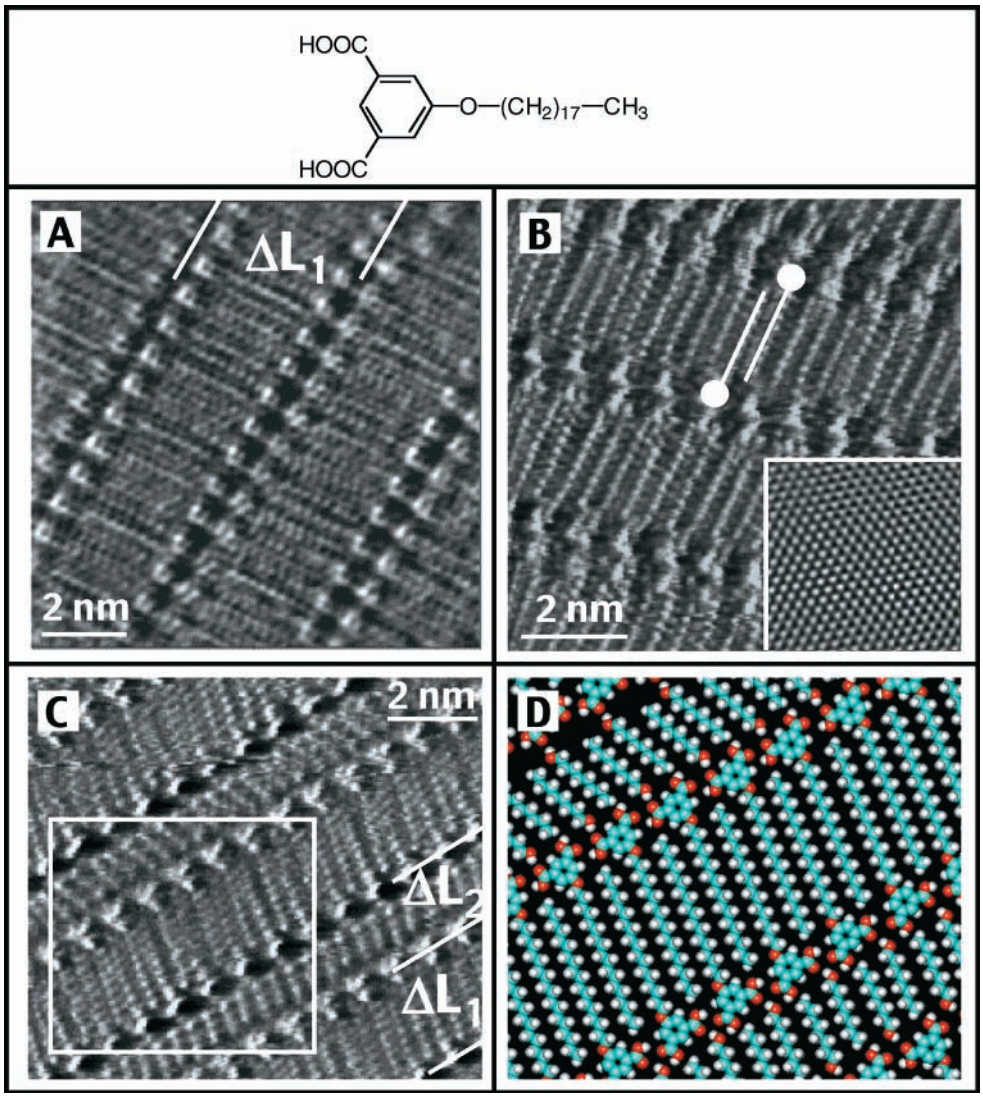

FIGURE 2. (A,B) Monolayers of **1** physisorbed from phenyloctane. (A) $I_{set} = 1.0$ nA, $V_{bias} \approx -0.7$ V. (B) $I_{set} = 1.0$ nA, $V_{bias} \approx -0.7$ V. The inset in (B) is a filtered image of the underlying graphite substrate. $I_{set} = 1.0$ nA, $V_{bias} \approx -0.1$ V. Filtering was performed to enhance the visual presentation. Two molecules are shown schematically. The circle corresponds to the isophthalic acid group, the line to the alkyl chain. (C) Monolayer of **1** physisorbed from 1-octanol ($I_{set} = 1.0$ nA, $V_{bias} = -1.3$ V); the corresponding model is shown in (D).

correspond to the alkyl groups, which are interdigitated over their full length and aligned with their long axis parallel to the graphite substrate and also parallel to a carbon chain on graphite (Figure 2B). This orientation of alkyl chains with respect to the graphite substrate is typical and is also observed for other compounds in this study. The graphite surface underneath the monolayer is imaged by reducing the bias voltage (reducing the tip−substrate distance) and is used for calibration purposes, taking into account that only one out of two graphite carbon atoms shows up in the STM image. ΔL_1 corresponds to the width of a lamella composed of **1**. The distance between adjacent isophthalic acid moieties allows for intermolecular hydrogen bonding. When isophthalic acid derivatives are dissolved in 1-octanol or 1-undecanol, solvent molecules are often incorporated in the monolayer. Figure 2C shows a monolayer formed by physisorption of **1** from 1-octanol which is characterized by alternating broad and small lamellae.[17] The broad lamellae (ΔL_1) are composed of **1**, while the small lamellae (ΔL_2) contain 1-octanol. The 1-octanol molecules are codeposited and are stabilized by hydrogen bonding. The formation of an alternating pattern of lamellae is unique, as other two-component systems show preferential segregation by formation of separate domains.[29]

Some functionalized hydrocarbons may display stabilizing hydrogen bonding along the lamella axis. For example, in monolayers of alkylated terephthalic acid derivatives such as 2,5-bis(dodecyloxy)terephthalic acid (**2**) (Figure 3A), the terephthalic acid groups (bright) are linked by hydrogen bonds, and the alkyl chains, which are oriented perpendicular to the lamella axis, are interdigitated (see model Figure 3B).

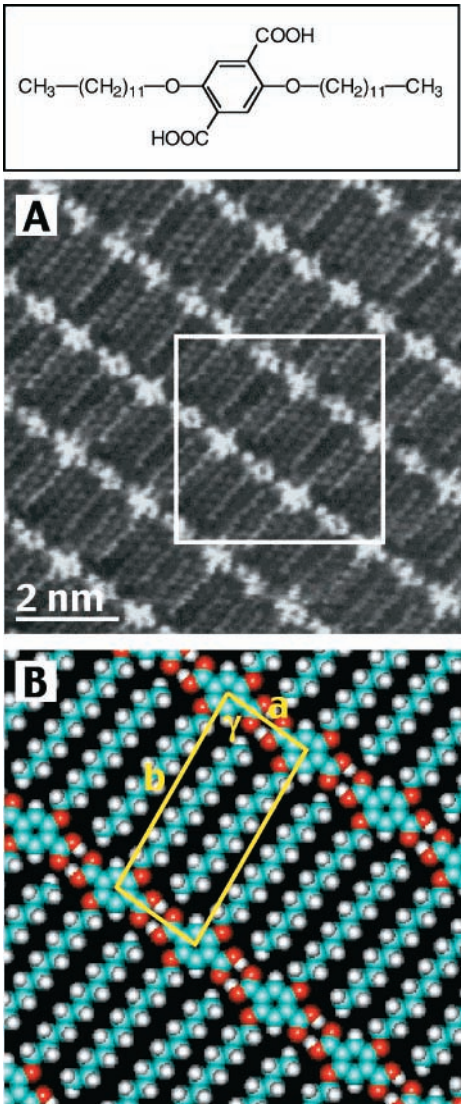

FIGURE 3. (A) STM image and (B) model of monolayer of **2**. I_{set} = 1 nA, $V_{bias} \approx -0.6$ V.

Chirality: Do Chiral Molecules Lead to Chiral Monolayers?

The ease of monolayer formation and their relative stability stimulated us to use isophthalic and terephthalic acid derivatives to study chirality, dynamics, and reactivity within physisorbed monolayers. Chiral molecules form a special class of "functionalized" molecules, and their effect on the two-dimensional ordering has recently received some attention. Stevens et al. reported the direct observation of enantiomorphous monolayer crystals from liquid crystalline enantiomers and the formation of coexisting enantiomorphous domains from a racemate by STM.[9,10] However, the stereogenic centers could not be visualized. The determination of the absolute chirality of individual adsorbed alkenes chemisorbed on the silicon surface has been demonstrated,[13] and recently, Fang et al. have determined the chirality of organic molecules by using a Br atom as a STM marker on the stereogenic center.[14] We have extended this research to the simultaneous analysis of chirality and conformation of a chiral terephthalic acid derivative[11] and to the study of the effect of chirality on the coadsorption process.[12] Figure 4A and B represents STM images of physisorbed monolayer structures of respectively (*S*)-**3**, the (*S*)-enantiomer, and (*R*)-**3**, the (*R*)-enantiomer of a chiral terephthalic acid derivative, 2,5-bis[10-(2-methylbutoxy)decyloxy]terephthalic acid (**3**), with two identical stereogenic centers.[11] The aromatic terephthalic acid groups appear as the larger bright spots. The monolayers are characterized by two different spacings between adjacent rows of (*R*)-**3** or (*S*)-**3** terephthalic acid groups. For both enantiomers, the width of the wide lamellae ($\Delta L_1 = 2.54 \pm 0.05$ nm) corresponds to the dimension of fully extended alkoxy chains, which are lying flat on the graphite surface and almost parallel to a main graphite axis. The width of the narrow lamellae ($\Delta L_2 = 1.9 \pm 0.1$ nm) indicates that the terminal 2-methylbutoxy groups are bent away from the surface, while the decyloxy groups are lying flat on the graphite surface, adopting an all-trans conformation. For this system, monolayer chirality is expressed in several ways. In regions of the monolayer where the alkoxy chains are fully extended, the STM images exhibit a clear modulation of the contrast along the lamellae. This superstructure (moiré pattern) is attributed to the incommensurability of the monolayer with the underlying graphite lattice.[25] The unit cells of this

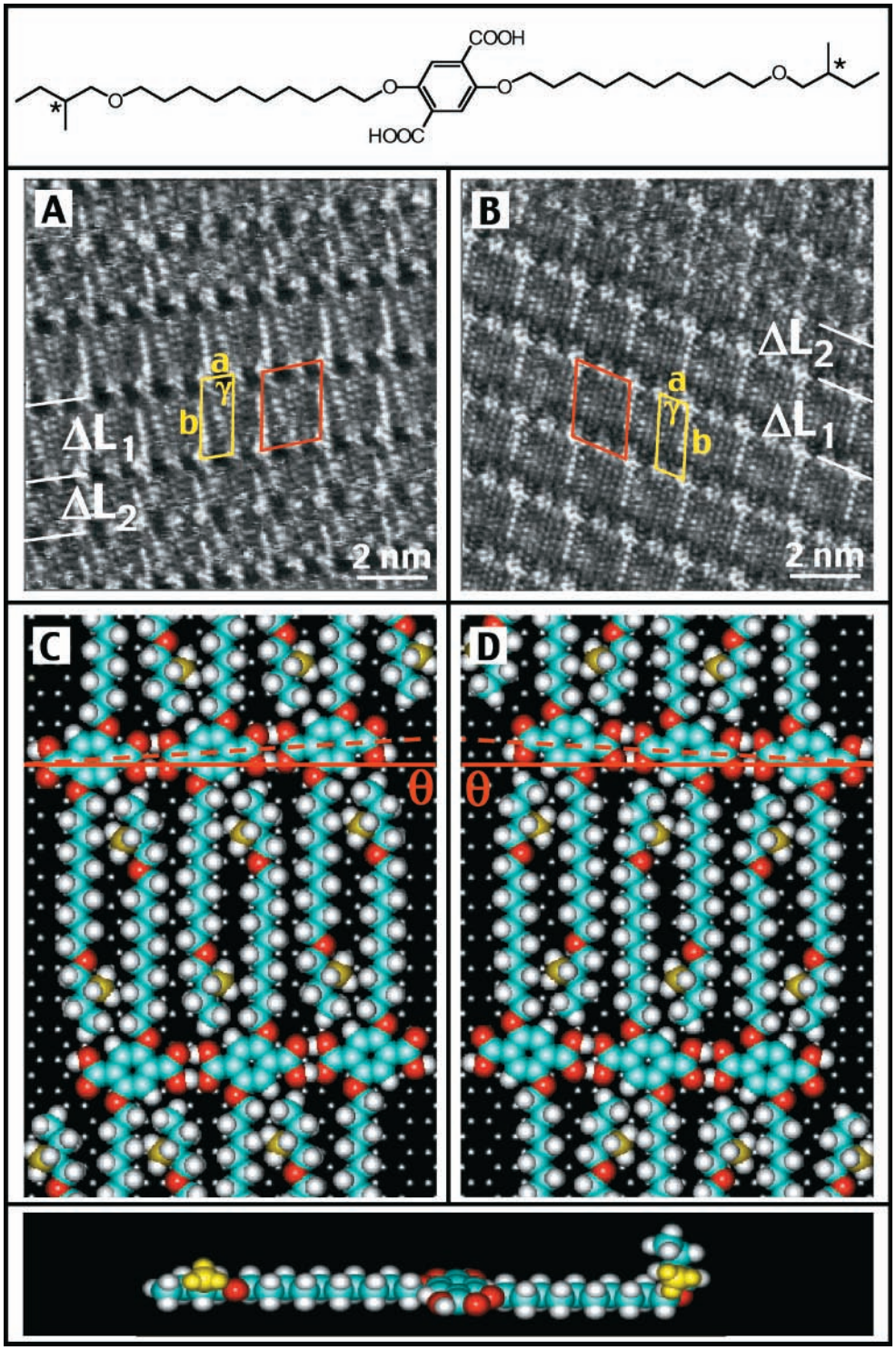

FIGURE 4. STM image and model of the (*S*)-enantiomer (A,C) (I_{set} = 0.5 nA, V_{bias} = −0.62 V) and the (*R*)-enantiomer (B,D) (I_{set} = 1.0 nA, V_{bias} = −0.47 V) domains of **3**. ΔL_1 and ΔL_2 indicate large lamellae (2-methylbutoxy groups adsorbed) and small lamellae (2-methylbutoxy groups pointing away from the surface), respectively. θ is the angle between the lamella axis and the graphite reference axis (see text). (Bottom) The alkoxy chain at the left of the model represents the extended conformation, while the 2-methylbutoxy component of the alkoxy group at the right is rotated out of plane.

contrast modulation, indicated in red, are mirror images for both enantiomers, which means that each enantiomer forms its characteristic enantiomorphous monolayer structure. This enantiomorphism is also expressed by the orientation of the lamella axes with respect to the graphite lattice: the angle θ between a lamella axis (any line parallel to a row formed by terephthalic acid groups) and a graphite reference axis, which is (nearly) perpendicular to the alkoxy chains, takes a value of $-3.7° \pm 0.3°$ and $+3.7° \pm 0.3°$ for a (*S*)-**3** (model Figure 4C) and a (*R*)-**3** domain (model Figure 4D), respectively. Note that the chirality of a domain is also expressed without making

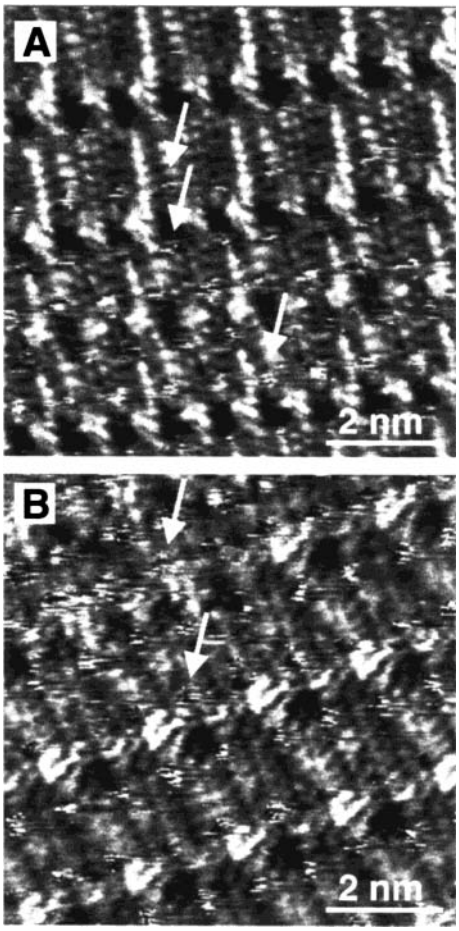

FIGURE 5. Monolayer images of the (*S*)-enantiomer (A) ($I_{set} = 0.5$ nA, $V_{bias} = -0.62$ V) and the (*R*)-enantiomer (B) ($I_{set} = 0.4$ nA, $V_{bias} = -0.37$ V) of **3**, revealing discontinuous features.

reference to the graphite surface underneath. However, for these systems, comparison of the monolayer orientation with the underlying graphite surface provides an elegant means for analysis.

In addition to the effect of chirality on the 2D ordering of these monolayers outlined above, Figure 5A and B, respectively, showing monolayer images of (*S*)-**3** and (*R*)-**3**, reveals elongated discontinuous features (arrows), both in narrow and wide lamellae. In the narrow lamellae, the position of those features can be identified with the location of 2-methylbutoxy groups, which are pointing away from the graphite surface. The discontinuous fuzzy character of the observed features is due to the mobility of the nonadsorbed chain ends and the interaction with the STM tip during the scanning process. However, these streaky features are also observed in the wide lamellae and are attributed to the interaction between the scanning tip and the protruding methyl unit on the tetrahedral stereogenic carbon atom, which allows visualization of the location of stereogenic centers in a *direct* way. Further support was provided by the observation that an increase of the bias voltage which results in a slight retraction of the tip only leads to the disappearance of the spots correlated with the stereogenic centers, while the spots related to the 2-methylbutoxy groups are still visible. Additional support was provided by the study of a reference compound, an achiral terephthalic acid derivative that also forms broad and small lamellae. Similar elongated structures appear only in the small lamellae, in agreement with the lack of stereogenic centers. Although the chiral terephthalic acid system demonstrates the expression of molecular chirality by the formation of distinct enantiomorphous domain structures by the respective enantiomers, a small percentage of the images displays domains reflecting the ordering expected for the other enantiomer. These aberrant arrangements, which will not be discussed in detail, can be accounted for by the presence of a small amount of impurities: achiral centrosymmetrical molecules which contain an (*S*)-stereogenic center on one alkoxy chain and an (*R*)-center on the other. Due to these complications, racemic solutions were not investigated in detail, and instead, the study of chiral isophthalic acid molecules was considered.

Figure 6A and B represents STM images of a monolayer of the (*S*)-enantiomer ((*S*)-**4**) and the (*R*)-enantiomer ((*R*)-**4**), respectively, of a chiral isophthalic acid derivative, 5-[10-(2-methylbutoxy)decyloxy]isophthalic acid (**4**), physisorbed from 1-heptanol.[12] The large spacing (ΔL_1) between adjacent rows of isophthalic acid groups corresponds to the dimension of extended and interdigitated aliphatic chains, while the smaller space (ΔL_2) is occupied by 1-heptanol molecules. The alkoxy groups are parallel to a row of carbon atoms of graphite, but the coadsorbed solvent molecules are not. The lamella axes form angles θ of $+3.5° \pm 0.7°$ ((*S*)-**5**) and $-3.8° \pm 0.6°$ ((*R*)-**4**) with the normal on the row of carbon atoms mentioned, or the normal on the alkoxy chains. As far as the packing of the isophthalic acid molecules is concerned, each enantiomer forms its characteristic enantiomorphous lamella structure. The orientation of both enantiomers with respect to the graphite surface is shown in Figure 6C,D. The orientation of the coadsorbed 1-heptanol molecules depends on the enantiomeric character of the domain in which those molecules are coadsorbed. For (*S*)-**4** monolayers, the alcohol molecules are rotated clockwise with respect to the normal on the isophthalic acid lamellae, while for (*R*)-**4** monolayers, this rotation is counterclockwise. As such, the orientation of *achiral* coadsorbed molecules expresses the chiral character of the domains.

In addition, a racemic solution has been investigated (Figure 7). The inset shows a magnification of the domain boundary. The left domain is negative ($\theta = -3.5°$) and the right domain is positive ($\theta = +3.5°$), and these domains reflect the ordering of (*R*)-**4** and (*S*)-**4** enantiomorphous monolayers, respectively. This suggests the separation of the enantiomers in different domains and, as such, reflects the Pasteur experiment in two dimensions.

It should be stressed that achiral molecules also form chiral domains. However, in contrast to an enantiomer, they form both mirror-type monolayer structures.

In summary, the "chiral" information of individual molecules is also expressed in the two-dimensional ordering of monolayers.

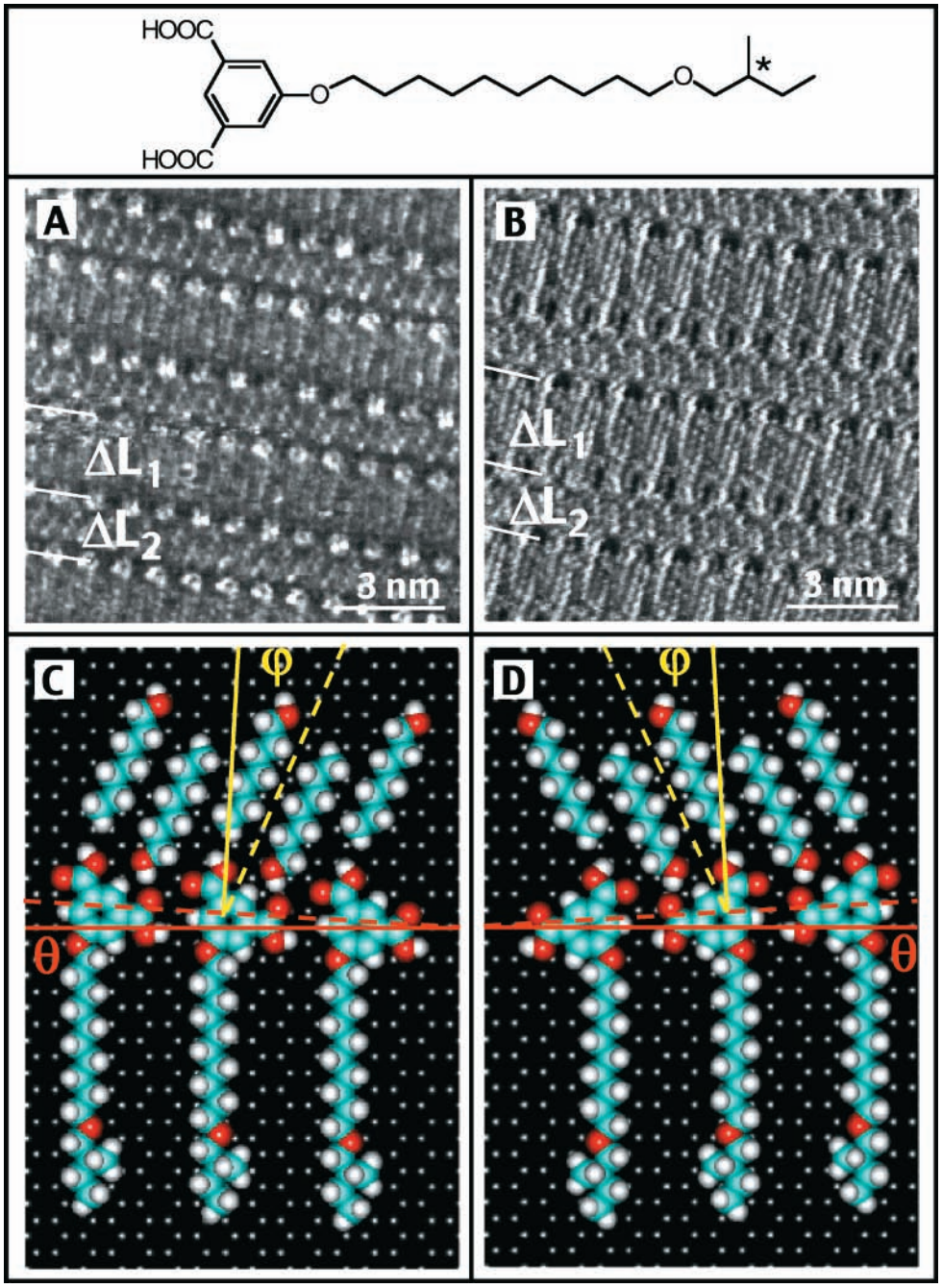

FIGURE 6. Monolayer image and model of the (*S*)-enantiomer (A,C) (I_{set} = 1.0 nA, $V_{bias} \approx -0.6$ V) and the (*R*)-enantiomer (B,D) (I_{set} = 0.5 nA, $V_{bias} = -0.45$ V) domains of **4**. ΔL_1 and ΔL_2 indicate lamellae composed of **4** and 1-octanol molecules, respectively. θ is the angle between the lamella axis and the graphite reference axis (see text). φ is the angle between the 1-octanol axis and the normal on the lamella axis of **4**.

Dynamics: a World of (Ex)change

A. Spontaneous Dynamics. Until now, we have considered only the time-averaged static characteristics of the physisorbed monolayers and neglected the dynamic character of these adlayers. The adlayers are still in contact with the supernatant solution and are subject to several dynamic phenomena. One should always take into account that the STM images are time averaged and the information concerning dynamics is limited by the image acquisition speed. In the following sections, we will demonstrate some of the (slow) dynamic processes.

The first example involves the reorientation of adsorbed molecules within the monolayer. Ostwald ripening describes the growth of larger domains at the expense of smaller domains. The thermodynamic driving force is the reduction of the circumference-to-area ratio and thereby the lowering of the interfacial or line energy. For example, application of nonsaturated solutions of 2-hexadecyl-9,-10-anthraquinone (**5**, Figure 8) in phenyloctane on HOPG leads to the formation of domains.[21] On a time scale of seconds, a small domain (A) shrinks until it disappears, while the larger domains (B,C) grow at its expense. After

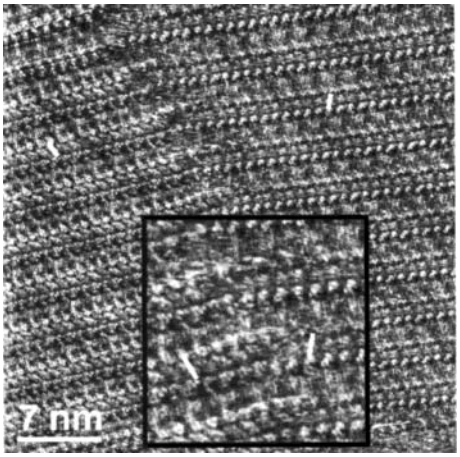

FIGURE 7. STM image of an ordered monolayer formed from a racemate solution of **4**. (Inset) An enlargement of part of the domain boundary. The left domain relects the ordering as found for pure (*R*)-enantiomer, while the right domain reflects the ordering of the (*S*)-enantiomer. The small bars reflect the orientation of some 1-octanol molecules. $I_{set} = 1.0$ nA, $V_{bias} \approx -0.7$ V.

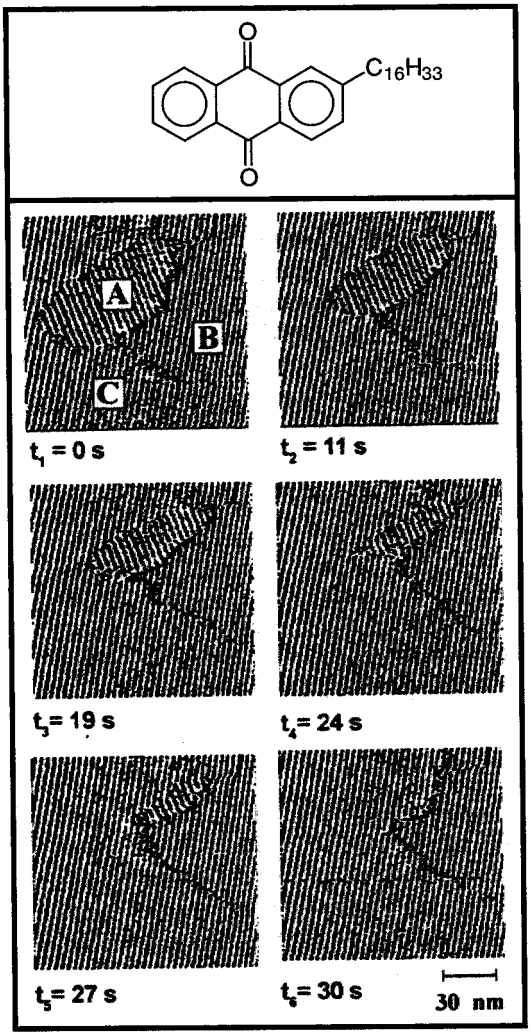

FIGURE 8. Series of STM images of compound **5** illustrating Ostwald ripening. $I_{set} = 1.5$ nA, $V_{bias} = -0.6$ V.

several minutes to a few hours, the 2D polycrystals become single crystalline on a micrometer scale. It was shown for this system that Ostwald ripening is determined

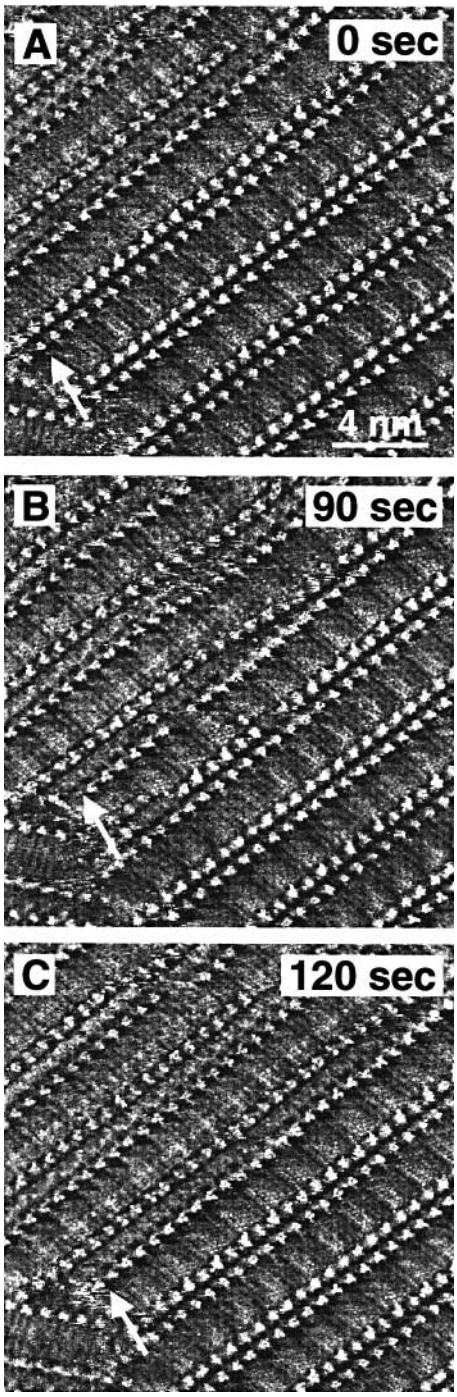

FIGURE 9. Codeposition dynamics of 1-octanol in a 5-eicosyloxyisophthalic acid monolayer. $I_{set} = 1.0$ nA, $V_{bias} = -0.8$ V.

by a reorientation of molecules at the domain boundaries of the 2D polycrystals. Indeed, at a domain boundary, molecules are often not ideally close packed, and the free volume within the 2D polycrystal is significantly increased. Therefore, individual molecules or lamella fragments at the domain boundary can change their orientation with respect to the underlying substrate without diffusing within the single crystals and without a transition to the supernatant solution.[5,33]

However, in a lot of cases, exchange of molecules with the supernatant solution gives rise to unique dynamics. For 5-alkoxyisophthalic acid derivatives, the codeposition

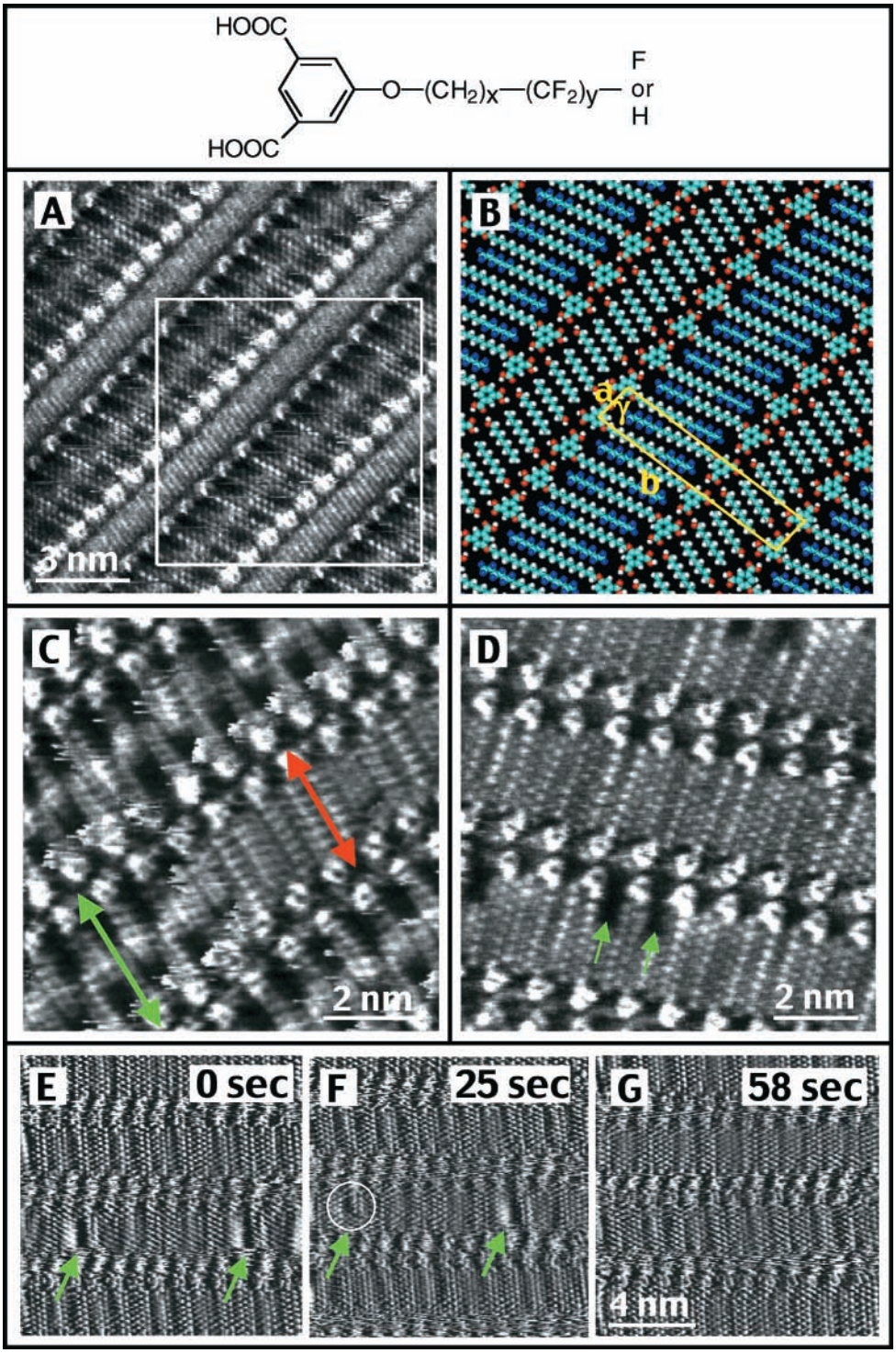

FIGURE 10. Monolayer image and model of H11F6 physisorbed from 1-octanol (A,B). The fluorinated parts appear dark (low tunneling current). I_{set} = 1.0 nA, V_{bias} = −0.7 V. (C) Segregation of H11F6 (green arrow) and H14F0 lamellae (red arrow). I_{set} = 1.0 nA, V_{bias} = −0.7 V. (D) Miscibility of H11F6 and H16F0 molecules. The green arrows indicate H11F6 molecules. I_{set} = 1.3 nA, V_{bias} = −1.35 V. (E−G) Snapshots of the desorption of H6F12 molecules in H18F0 lamellae. The H6F12 molecules are indicated by arrows. The circle in (F) indicates a molecule with an apparent smaller fluorinated part. This is caused by desorption of an H6F11 molecule while the tip was scanning over the molecule. I_{set} = 1.1 nA, V_{bias} = −0.38 V.

process of 1-octanol molecules could be followed (Figure 9).[27] This image sequence visualizes the insertion of 1-octanol molecules between two isophthalic acid lamellae. A domain boundary at the left (arrow) is used as a reference point. The insertion process is completed within 2 min and involves the adsorption of ∼48 1-octanol molecules. Not surprisingly, this process is initiated at a domain boundary, typically a region with lower stability and enhanced dynamics. Codeposition involves the exchange of molecules with the supernatant solution and reorientation (translation) of large monolayer parts in a cooperative fashion. For instance, the lamellae in the

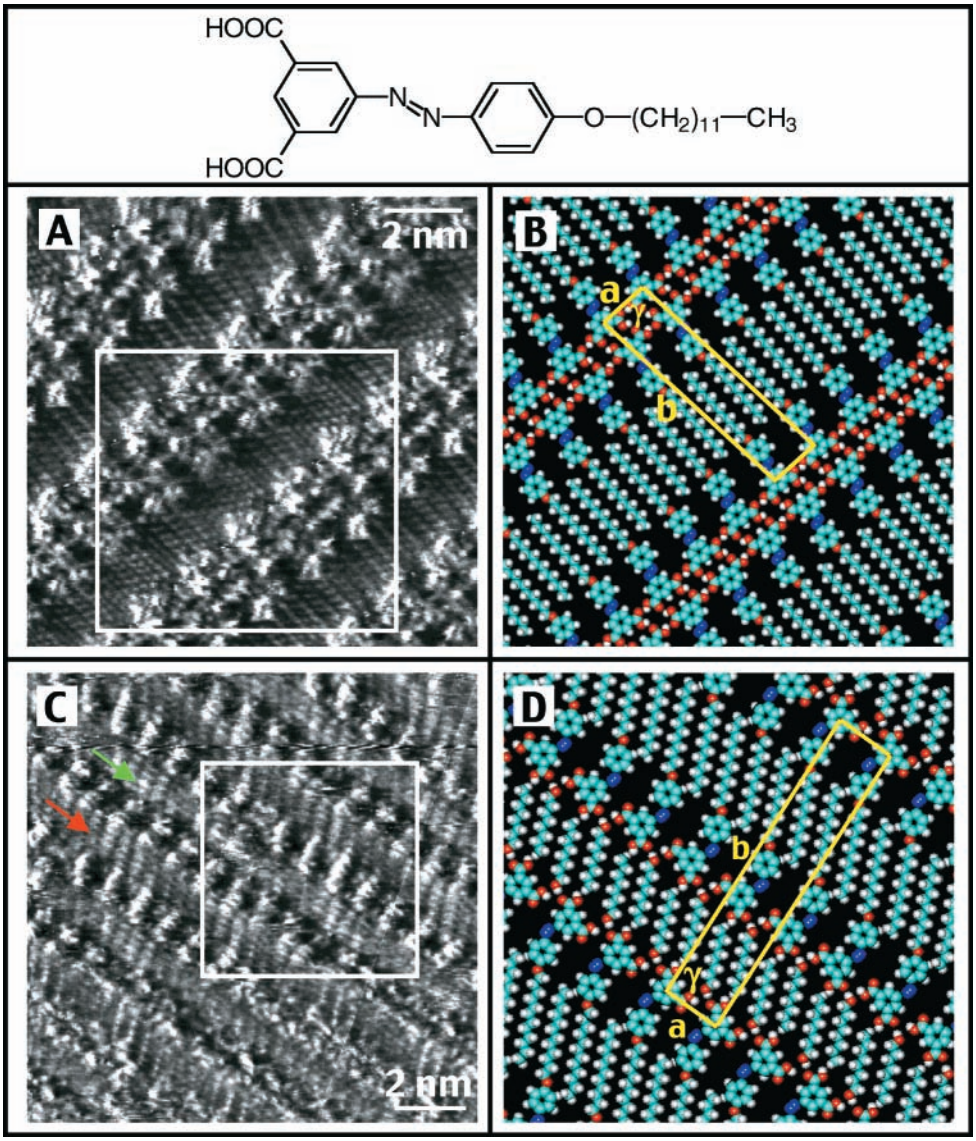

FIGURE 11. Trans−cis isomerization of **6**. Monolayer image (A) and model (B) of *trans*-**6**. Monolayer image (C) and model (D) of *cis*-**6**. The green arrow indicates a lamella of 1-octanol molecules. The red arrow indicates a *cis*-**6** lamella.

upper half of the image are translated during the insertion process, and this is expressed by the appearance of a "wavelike" pattern. The lamellae in the lower half of the image are rather unaffected by the insertion process.

These experiments clearly illustrate the dynamics and structural changes that take place spontaneously within monolayers at the solid−fluid interface. However, they do not provide information about the exchange or mobility of individual molecules in domains that do not undergo major structural changes. In view of this, we introduced semifluorinated isophthalic acid derivatives, which can act as markers that allow us to study this type of dynamics. Figure 10A represents a monolayer of H11F6 (ISA−$(CH_2)_{11}$−$(CF_2)_6$−F) physisorbed from 1-octanol and displays the typical ordering found for most isophthalic acid derivatives studied (model Figure 10B).[26] The perfluorinated part of the alkyl chain can be clearly distinguished as a black band, due to the decreased tunneling current. For mixed solutions of semifluorinated and nonfluorinated isophthalic acid derivatives, it was observed that whether or not segregation takes place depends upon the difference in length between the semifluorinated and nonfluorinated molecules. Formation of separate lamellae was observed for those systems, which differ in length by three methylene units (e.g., H11F6 and H14F0, Figure 10C).[26] If there is no difference in chain length or if the length differs only by one methylene group, mixed monolayers are formed (e.g., H11F6 and H16F0, Figure 10D)[26] and individual semifluorinated molecules are dispersed in a matrix formed by the nonfluorinated ones. With a fast scanning STM (2 frames/s), it was observed that semifluorinated molecules desorb and are replaced by nonfluorinated ones (H6F12 and H18F0, Figure 10E−G).[27] The residence time of single fluorinated molecules is on the order of seconds to several minutes, much longer than the estimated residence time reported for mixtures of saturated/unsaturated acids and alcohol/thiol mixtures by Stevens et al.[30] When solvent effects are neglected, this can partially be accounted for by the stabilizing effect of isophthalic acid hydrogen bonding.

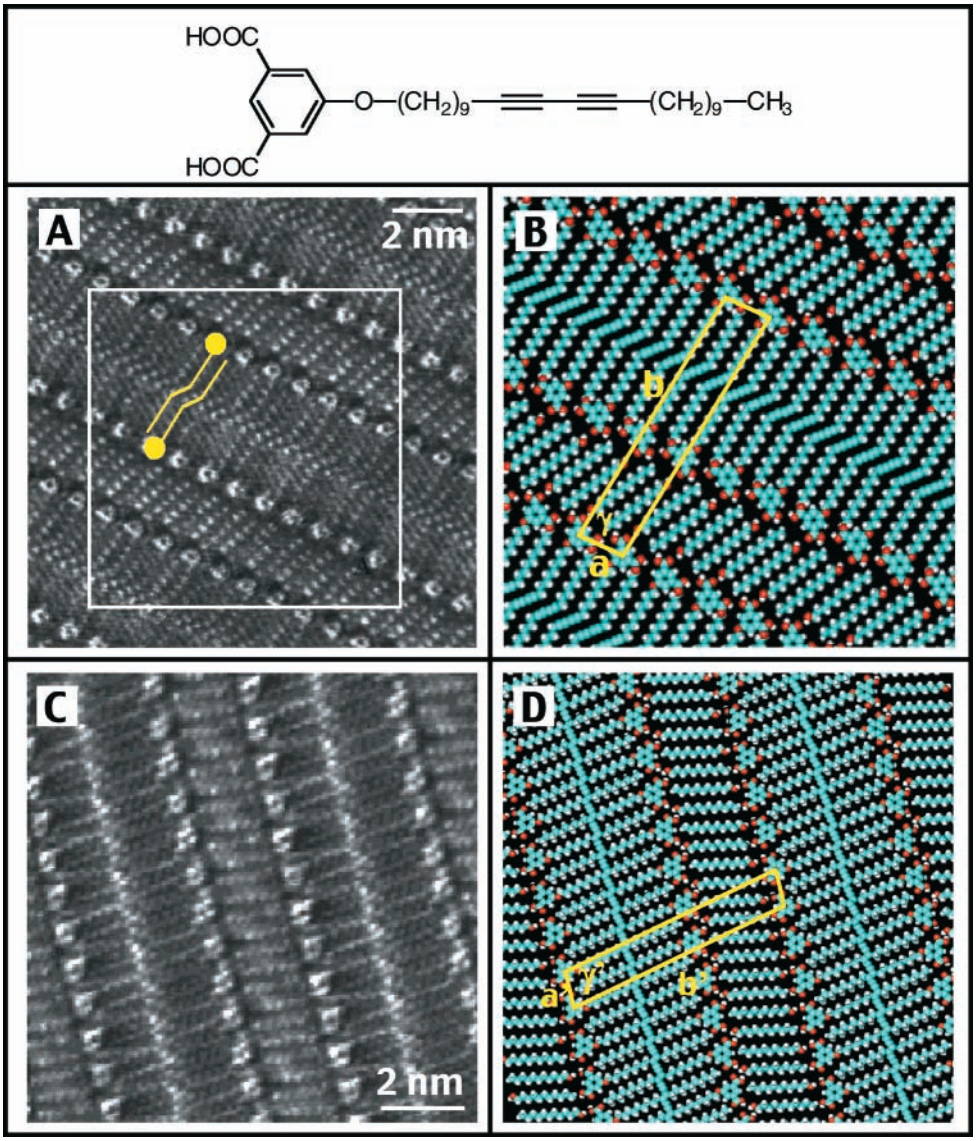

FIGURE 12. Topological polymerization of **8**. Monolayer image and model of unpolymerized product physisorbed from 1-undecanol (A,B). I_{set} = 1.0 nA, V_{bias} = −1.2 V. Monolayer image and model of polymerized product (C,D) after illumination. I_{set} = 1.0 nA, V_{bias} = −0.5 V.

B. Triggering of Dynamics. In addition to dynamic processes, which occur spontaneously at the liquid−solid interface, monolayer changes can also be induced by external stimuli such as heating,[34] electrochemical changes,[35] and light.[16−20] We have investigated the light-induced changes for a couple of photoreactive systems. With the aim of imaging the starting material and the reaction product of a reversible photoreaction, the cis−trans isomerization of an azoisophthalic acid derivative (**6**) was investigated. Figure 11A,B shows a STM image and model of a monomolecular layer of *trans*-**6** physisorbed from 1-undecanol and shielded from light. The distinct bright bands correspond to the azobenzene moieties. Dimers are formed by hydrogen bonding, and the alkyl chains are interdigitated. Codeposition of solvent molecules was not observed. Figure 11C shows a STM image of a monolayer obtained by physisorption from a photostationary mixture after illumination of the solution in a cuvette (ex situ) at 366 nm. In addition to the regular monolayer structure characteristic for *trans*-**6**, a new monolayer structure appeared which was never before observed for *trans*-**6** monolayers. The distances and the observed molecular packing correspond to a monolayer of self-assembled *cis*-**6** with codeposition of 1-octanol molecules (Figure 11D). It was not possible to form adlayers, which solely show the *cis*-**6** monolayer structure. This can be attributed to the photostationary character of the mixture and to the larger affinity of *trans*-**6** compared to *cis*-**6** to form monolayers on the graphite surface. In general, cis regions are less stable than trans regions, and it was not possible to visualize *cis*-**6** monolayers after in situ illumination (illumination of the solution on graphite without scanning).

However, formation of cis domains after in situ illumination was realized for an isophthalic acid derivative with an azobenzene moiety as part of the side chain.[17] A possible mechanism for replacement of physisorbed "reactant" molecules by the "product" initiated by in situ

illumination is the following. Irradiation of the system will lead to a change of the equilibrium composition and a concentration gradient in the supernatant solution. A decrease in trans concentration will induce desorption and enhance the adsorption of cis molecules. In addition, the isomerization reaction could also occur on the graphite surface itself and initiate the cis product domain formation, although this is expected to contribute only to a minor extent due to steric hindrance. During imaging (illumination off), these cis domains disappear with time until finally only trans isomer domains remain, due to the thermal back reaction (cis to trans).

In addition to a reversible cis−trans isomerization, an irreversible photoreaction was studied: the phototransformation of 10-diazo-2-hexadecylanthrone (**7**) to 2-hexadecyl-9,10-anthraquinone (**5**).[16] Irradiation leads to the dissolution of the highly ordered molecular pattern of **7**, starting at a domain boundary. When the irradiation is stopped, the highly ordered pattern reappeared, and recrystallization of molecules of type **7** occurred. As described in the previous section, the desorption must be the result of the formation of a concentration gradient induced by illumination. When irradiation is stopped, the system relaxes and the 2D crystal is reformed. Only when all reactant was transformed to product, which occurred after several illumination cycles, were monolayers of **5** formed.

Both phototransformations are believed to take place predominantly in the supernatant solution. To demonstrate the possibility of reactivity *within* the physisorbed monolayer, the study of a topological reaction was considered: the photopolymerization of diacetylene,[18] for which it is known that the relative orientation of the diacetylene groups is critical. The molecule chosen in this study is the diacetylene-containing isophthalic acid derivative (**8**, Figure 12**)**. This compound forms a physisorbed monolayer spontaneously at the liquid−graphite interface from a 1-undecanol solution (Figure 12A). The structure consists of lamellae of **8** alternated by solvent lamellae. The diacetylene moieties appear as bright spots in the middle of the lamellae. Within a lamella, the distance between isophthalic acid groups is 9.44 ± 0.09 Å. The alkyl chains of **8** are lying parallel to the substrate in the direction of one of the main graphite axes, and the orientation is modeled in Figure 12B. After in situ illumination (254 nm, no scanning) of the monolayer film on graphite, the surface was reexamined, using the same scanning parameters as those used prior to the illumination, and again monolayer structures were observed (Figure 12C). Isophthalic acid groups and solvent molecules are well resolved. The contrast in the middle of a lamella can be described by a series of bright spots, clearly distinct from individual acetylene units, which suggests that the monolayer structure might be polymerized along the lamella direction. The most important change in the monolayer structure, however, is the change in spacing between the isophthalic acid groups. The distance was determined to be 9.81 ± 0.05 Å, in contrast to the unpolymerized repeating distance of 9.44 ± 0.09 Å. A molecular model for a polymerized monolayer structure is shown in Figure 12D. The experimental value of 9.81 Å for the isophthalic acid group distance is in perfect accord with the value of 9.82 Å obtained for a model optimized for the polymer chain. Consequently, the repeating distance in the polymer backbone is 4.91 Å, which is in agreement with the three-dimensional crystal structure data of polymerized diacetylenes.[36] The structural parameters, describing the orientation of adjacent diacetylene units in unpolymerized monolayers, correspond to those values for which it was experimentally shown by X-ray crystallography that crystallized diacetylene monomers could polymerize.[36]

Conclusion

In conclusion, STM provides a unique approach to the study of physisorbed organic monolayers. Due to the local nature of probing, very detailed information can be obtained, not only on the static properties (structure, contrast) but also on the dynamics (spontaneous or (light-)induced) of physisorbed monolayers. Due to its versatility, STM will continue to be an excellent probe to provide more information on a submolecular scale on the ordering, dynamics, and reactivity at interfaces.

The authors thank the DWTC, through IUAP-IV-11, and ESF SMARTON for financial support. S.D.F. thanks the Fund for Scientific Research−Flanders for financial support. A.G. thanks the IWT for a predoctoral scholarship. The collaboration was made possible thanks to the TMR project SISITOMAS.

References

(1) Binnig, G.; Rohrer, H.; Gerber, C.; Weibel, E. Surface Studies by Scanning Tunneling Microscopy. *Phys. Rev. Lett.* **1982**, *49*, 57−61.
(2) Binnig, G.; Rohrer, H.; Scanning Tunneling Microscopy−from birth to adolescence. *Rev. Mod. Phys.* **1987**, *59*, 615−625.
(3) Foster, J. S.; Frommer, J. E. Imaging of Liquid Crystals Using a Tunneling Microscope. *Nature* **1988**, *333*, 542−545.
(4) McGonigal, G. C.; Bernhardt, R. H.; Thomson, D. J. Imaging Alkane Layers at the Liquid/Graphite Interface with the Scanning Tunneling Microscope. *Appl. Phys. Lett.* **1990**, *57*, 28−30.
(5) Rabe, J.; Buchholz, S. Commensurability and Mobility in Two-Dimensional Molecular Patterns on Graphite. *Science* **1991**, *253*, 424−427.
(6) Frommer, J. Scanning Tunneling Microscopy and Atomic Force Microscopy in Organic Chemistry. *Angew. Chem., Int. Ed. Engl.* **1992**, *31*, 1298−1328.
(7) Cyr, D. M.; Venkataraman, B.; Flynn, G. W. STM investigations of Organic Molecules Physisorbed at the Liquid−Solid Interface. *Chem. Mater.* **1996**, *8*, 1600−1615.
(8) Giancarlo, L. C.; Flynn, G. W. Scanning Tunneling and Atomic Force Microscopy Probes of Self-Assembled, Physisorbed Monolayers. *Annu. Rev. Phys. Chem.* **1998**, *49*, 297−336.
(9) Stevens, F.; Dyer, D. J.; Walba, D. M. Direct Observation of Enantiomorphous Monolayer Crystals from Enantiomers by Scanning Tunneling Microscopy. *Angew. Chem., Int. Ed. Engl.* **1996**, *35*, 900−901.
(10) Walba, D. M.; Stevens, F.; Clark, N. A.; Parks, D. C. Detecting Molecular Chirality by Scanning Tunneling Microscopy. *Acc. Chem. Res.* **1996**, *29*, 591−597.
(11) De Feyter, S.; Gesquière, A.; Grim, P. C. M.; De Schryver, F. C.; Valiyaveettil, S.; Meiners, C.; Sieffert, M.; Müllen, K. Expression of Chirality and Visualization of Stereogenic Centers by Scanning Tunneling Microscopy. *Langmuir* **1999**, *15*, 2817−2822.
(12) De Feyter, S.; Grim, P. C. M.; Rücker, M.; Vanoppen, P.; Meiners, C.; Sieffert, M.; Valiyaveetiil, S.; Müllen, K.; De Schryver, F. C. Expression of Chirality by Achiral Coadsorbed Molecules in Chiral Monolayers Observed by STM. *Angew. Chem., Int. Ed.* **1998**, *37*, 1223−1226.

(13) Lopinski, G. P.; Moffatt, D. J.; Wayner, D. D. M.; Wolkow, R. A. Determination of the Absolute Chirality of Individual Adsorbed Molecules using the Scanning Tunneling Microscope. *Nature* **1998**, *392*, 909−911.
(14) Fang, H.; Giancarlo, L. C.; Flynn, G. W. Direct Determination of the Chirality of Organic Molecules by Scanning Tunneling Microscopy. *J. Phys. Chem. B* **1998**, *102*, 7311−7315.
(15) Böhringer, M.; Morgenstern, K.; Schneider, W.-D.; Berndt, R. Separation of a Racemic Mixture of Two-Dimensional Molecular Clusters by Scanning Tunneling Microscopy. *Angew. Chem., Int. Ed.* **1999**, *38*, 821−823.
(16) Heinz, R.; Stabel, A.; Rabe, J. P.; Wegner, G.; De Schryver, F. C.; Corens, D.; Dehaen, W.; Süling, C. Photodecomposition of 10-Diazo-2-hexadecyl-anthrone on Graphite Studied by Scanning Tunneling Microscopy. *Angew. Chem., Int. Ed. Engl.* **1994**, *33*, 2080−2082.
(17) Vanoppen, P.; Grim, P. C. M.; Rücker, M.; De Feyter, S.; Moessner, G.; Valiyaveettil, S.; Müllen, K.; De Schryver, F. C. Solvent Codeposition and Cis−Trans Isomerization of Isophthalic Acid Derivatives Studied by STM. *J. Phys. Chem.* **1996**, *100*, 19636−19641.
(18) Grim, P. C. M.; De Feyter, S.; Gesquière, A.; Vanoppen, P.; Rücker, M.; Valiyaveettil, S.; Moessner, G.; Müllen, K.; De Schryver, F. C. Submolecularly Resolved Polymerization of Diacetylene Molecules on the Graphite Surface Observed with Scanning Tunneling Microscopy. *Angew. Chem., Int. Ed. Engl.* **1997**, *36*, 2601−2603.
(19) Takami, T.; Ozaki, H.; Kasuga, M.; Tsuchiya, T.; Mazaki, Y.; Fukushi, D.; Ogawa, A.; Uda, M. Periodic Structure of a Single Sheet of a Clothlike Macromolecule (Atomic Cloth) Studied by Scanning Tunneling Microscopy. *Angew. Chem., Int. Ed. Engl.* **1997**, *36*, 2755−2757.
(20) Grim, P. C. M.; Vanoppen, P.; Rücker, M.; De Feyter, S.; Valiyaveettil, S.; Moessner, G.; Müllen, K.; De Schryver, F. C. Molecular Organization of Azobenzene Derivatives at the Liquid/Graphite Interface Observed with Scanning Tunneling Microscopy. *J. Vac. Sci. Technol. B* **1997**, *15*, 1419−1424.
(21) Stabel, A.; Heinz, R.; De Schryver, F. C.; Rabe, J. P. Ostwald Ripening of Two-Dimensional Crystals at the Solid−Liquid Interface. *J. Phys. Chem.* **1995**, *99*, 505−507.
(22) Venkataraman, B.; Breen, J. J.; Flynn, G. W. Scanning Tunneling Microscopy Studies of Solvent Effects on the Adsorption and Mobility of Triacontane/Triacontanol Molecules Adsorbed on Graphite. *J. Phys. Chem.* **1995**, *99*, 6608−6619.
(23) Buchholz, S.; Rabe, J. P. Conformation, Packing, Defects, and Molecular Dynamics in monolayers of Dialkyl-Substituted Benzenes. *J. Vac. Sci. Technol. B* **1991**, *9*, 1126−1128.
(24) Adkadskaya, L.; Rabe, J. P. Anisotropic Molecular Dynamics in the Vicinity of Order-Disorder Transitions in Organic Monolayers. *Phys. Rev. Lett.* **1992**, *69*, 1395−1398.
(25) Stabel, A.; Heinz, H.; Rabe, J. P.; Wegner, G.; De Schryver, F. C.; Corens, D.; Dehaen, W.; Süling, C. STM Investigation of 2D Crystals of Anthrone Derivatives on Graphite: Analysis of Molecular Structure and Dynamics. *J. Phys. Chem.* **1995**, *99*, 8690−8697.
(26) Gesquière, A.; Abdel-Mottaleb, M.; De Schryver, F. C. Imaging of a Fluorine Substituted Isophthalic Acid Derivative on Graphite with Scanning Tunneling Microscopy. *Langmuir* **1999**, *15*, 6821−6824.
(27) Gesquière, A.; Abdel-Mottaleb, M.; De Feyter, S.; De Schryver, F. C.; Sieffert, M.; Müllen, K.; Calderone, A.; Lazzaroni, R.; Brédas, J. L. Dynamics in Physisorbed Monolayers of 5-Alkoxy-Isophthalic Acid Derivatives at the Liquid/Solid Interface Investigated by Scanning Tunneling Microscopy. *Chem. Eur. J.*, in press.
(28) De Feyter, S.; Grim, K.; van Esch, J.; Kellogg, R. M.; Feringa, B. L.; De Schryver, F. C. Non-Trivial Differentiation between Two Identical Functionalities within the Same Molecule Studied by STM. *J. Phys. Chem. B* **1998**, *102*, 8981−8987.
(29) Baker, T. R.; Mougous, J. D.; Brackley, A.; Patrick, D. L. Competitive Adsorption, Phase Segregation, and Molecular Motion at a Solid−Liquid Interface Studied by Scanning Tunneling Microscopy. *Langmuir* **1999**, *15*, 4884−4891.
(30) Stevens, F.; Beebe, T. P. Dynamical Exchange Behavior in Organic Monolayers Studied by STM Analysis of Labeled Mixtures. *Langmuir* **1999**, *15*, 6884−6889.
(31) Claypool, C. L.; Faglioni, F.; Goddard, W. A., III; Gray, H. B.; Lewis, N. S.; Marcus, R. A. Source of Image Contrast in STM images of Functionalized Alkanes on Graphite: A Systematic Functional Group Approach. *J. Phys. Chem. B* **1997**, *101*, 5978−5995.
(32) Faglioni, F.; Claypool, C. L.; Lewis, N. S.; Goddard, W. A., III. Theoretical Description of the STM Images of Alkanes and Substituted Alkanes Adsorbed on Graphite. *J. Phys. Chem. B* **1997**, *101*, 5996−6020.
(33) Rabe, J. P.; Buchholz, S. Direct Observation of Molecular Structure and Dynamics at the Interface between a Solid Wall and an Organic Solution by Scanning Tunneling Microscopy. *Phys. Rev. Lett.* **1991**, *66*, 2096−2099.
(34) Bucher, J.-P.; Roeder, H.; Kern, K. Thermally Induced Disorder and Conformational Defects of Alkane Monolayers on Graphite. *Surf. Sci.* **1993**, *289*, 370−380.
(35) Tao, N. J.; Shi, Z. Real-Time STM/AFM Study of Electron Transfer Reactions of an Organic Molecule: Xanthine at the Graphite−Water Interface. *Surf. Sci.* **1994**, *321*, L149-L156.
(36) Enkelmann, V. Structural Aspects of the Topochemical Polymerization of Diacetylenes. *Adv. Polym. Sci.* **1984**, *63*, 91−136.

AR970040G